QUANTUM INTERFEROMETRIC OPTICAL LITHOGRAPHY: EXPLOITING ENGANGLEMENT TO BEAT THE DIFFRACTION LIMIT

Agedi N. Boto, Daniel S. Abrams, Colin P. Williams, and Jonathan P. Dowling*

Quantum Computing Technologies Group, Section 367
Jet Propulsion Laboratory, California Institute of Technology
Mail Stop 126-347, 4800 Oak Grove Drive, Pasadena, California 91109

(Received:)

Classical, interferometric, optical lithography is diffraction limited to writing features of a size $\lambda/4$ or greater, where λ is the optical wavelength. Using nonclassical photon-number states, entangled N at a time, we show that it is possible to write features of minimum size $\lambda/(4N)$ in an N-photon absorbing substrate. This result surpasses the usual classical diffraction limit by a factor of N. Since the number of features that can be etched on a two-dimensional surface scales inversely as the square of the feature size, this allows one to write a factor of N^2 more elements on a semiconductor chip. A factor of $N = 2$ can be achieved easily with entangled photon pairs generated from optical parametric downconversion.

PACS: 42.50.H, 85.40.H, 42.25.H, 42.65.K

---

02 DEC 99, Ver. 1.2, to be submitted to *Phys. Rev. Lett.*

* Electronic address: Jonathan.P.Dowling@jpl.nasa.gov

Optical masking lithography has been the primary tool of the semiconductor industry for transferring circuit images onto substrates to form semiconductor chips. However, diffraction edge effects in the typical masking approach limits the minimal resolvable feature size to about the Rayleigh diffraction limit of $\lambda/2$, where λ is the optical wavelength. Hence, it has become necessary to use light of ever-shorter wavelengths to fabricate smaller features. Current production technology writes 180–220 nm features using KrF excimer laser light at 248 nm. New technological approaches consider light in the vacuum ultraviolet or soft x ray regime in order to obtain features at 100 nm or below [1]. In all cases, the light is treated classically or, equivalently, as a stream of uncorrelated photons—an approach that leads to the Rayleigh criterion of $\lambda/2$ as an apparently inviolable diffraction limit. We shall demonstrate that it is possible to overcome this limit by using entangled photons, which have no classical analog.

A factor of two improvement over the limit of $\lambda/2$ can be achieved using classical interferometric lithography (CIL) [2]. In CIL, when two coherent plane waves of laser radiation are made to intersect at an angle of 2θ, as shown in Fig. (1), interference fringes form with a spacing or pitch of $p = \lambda/2 \sin \theta$. In the grazing incidence limit as $\theta \rightarrow \pi/2$, the minimum linear feature size $x^{\min}$ that can be written is $x^{\min} = \lambda/4$. To see this, realize that the normalized exposure dose Δ at the substrate (proportional to the intensity) is given by the scaled interference pattern of two counter-propagating, grazing incidence, plane waves, $\Delta(x) =$

$1 + \cos(2kx) = 1 + \cos\varphi$. Here, $k = 2\pi/\lambda$ is the optical wavenumber, $\varphi = 2kx$ is the associated path-differential phase, and x the lateral dimension on the substrate. (We shall assume the optimal grazing incidence $\theta \to \pi/2$ for the rest of this work.) The Rayleigh criterion states that the minimal resolvable feature size occurs at a spacing corresponding to the distance between an intensity maximum and an adjacent intensity minimum [3]. The criterion then demands $\varphi^{\min} = \pi$, from which we obtain $x^{\min} = \lambda/4$, as given above. This is the best resolution that can be achieved classically through uncorrelated, single-photon, interferometric techniques [2].

Recently, Yablonovitch and Vrijen (YV) have proposed utilizing "classical" two-photon exposure techniques to improve lithographic resolution. The idea is that uncorrelated (classical) two-photon absorption probability scales quadratically with the classical intensity [4]. Hence, in our interferometric setting, the two-photon exposure dose $\Delta_{2\gamma}$ has the form, $\Delta_{2\gamma} = \Delta^2(x)/2 = (1+\cos\varphi)^2/2 = \frac{3}{4} + \cos\varphi + \frac{1}{4}\cos 2\varphi$. This function has a term $\frac{1}{4}\cos 2\varphi$ that oscillates in space with twice the frequency as the single-photon function, $\Delta(x)$. If the middle term containing the more slowly oscillating $\cos\varphi$ could somehow be removed, one would be left with only the high spatial-frequency pattern term, of resolution $x_{2\gamma}^{\min} = \lambda/8$. Since the number of elements writeable on a surface scales quadratically with the minimum feature dimension, this is an important advance. The approach of YV is to delete this middle term using classical frequency modulation. In the rest of this work, we show instead how to employ entangled photons,

in a quantum interferometric setting, to selectively delete this middle term and achieve a resolution at half the classical diffraction limit.

It has been known for some time that entangled photon pairs, such as those generated by spontaneous parametric down conversion (PDC) [4], have unusual imaging and resolving characteristics. This feature allows for sub-shot-noise interferometric phase measurement in theory [5, 6] and experiment [7]. In fact, Fonseca, *et al.,* recently demonstrated resolution of a two-slit diffraction pattern at half the Rayleigh limit in a coincidence-counting experiment [7]. What we will now show is that this type of effect is possible not only in coincidence experiments, but also in real two-photon imaging systems such as those used in classical interferometric lithography. In particular, we will demonstrate that quantum entanglement is the resource that allows sub-diffraction-limited lithography.

Consider the schematic set up for interferometric lithography, illustrated in Fig. (1). We consider a two-port device with photons incident on a symmetric, lossless, beam splitter from the left in one or both ports A or B. The photons are then reflected by a mirror pair (M) onto the imaging plane of the system at the right. Without loss of generality, we can model the phase differential due to path-length differences between the upper and lower branches of the interferometer as a single phase shifter (PS) placed in the upper branch, which imparts a phase shift $\varphi = 2kx$. The two photon paths converge on the imaging plane at an angle of θ off the horizontal axis, as show in the figure. We identify with the two input ports A and B at the left, two photon annihilation operators $\hat{a}$ and $\hat{b}$, respectively [6]. These operators and their Hermitian conjugates, $\hat{a}^{\dagger}$ and $\hat{b}^{\dagger}$, obey the usual photon

commutation rules, $\left[\hat{a},\hat{a}^{\dagger}\right]=\left[\hat{b},\hat{b}^{\dagger}\right]=1$ and $\left[\hat{a},\hat{b}\right]=\left[\hat{a},\hat{b}^{\dagger}\right]=0$. We can take the output electric field operator at the image plane on the right to be proportional to the sum of two output operators $\hat{c}$ and $\hat{d}$ from the upper and lower branches of the interferometer, C and D, respectively. Then the linear relationship between the two inputs and the two outputs can be expressed by a two-dimensional matrix equation, $\hat{\mathbf{T}}\begin{bmatrix}\hat{a}\\ \hat{b}\end{bmatrix}=\begin{bmatrix}\hat{c}\\ \hat{d}\end{bmatrix}$, where $\hat{\mathbf{T}}$ is the input-output transfer matrix. For our purposes, $\hat{\mathbf{T}}$ can be thought of as being the product of matrices of the form,

$$\hat{\mathbf{B}}=\frac{1}{\sqrt{2}}\begin{pmatrix}-1 & i\\ i & -1\end{pmatrix},\qquad \hat{\mathbf{R}}=\begin{pmatrix}-1 & 0\\ 0 & -1\end{pmatrix},\qquad \hat{\mathbf{P}}=\begin{pmatrix}e^{i\varphi} & 0\\ 0 & 1\end{pmatrix}, \tag{1}$$

which represent the unitary actions of the symmetric lossless beam splitter (BS), the mirror pair (M), and the phase shifter (PS), respectively. Here, we have assumed a π phase shift on each reflection off of a BS or a mirror and a $\pi/2$ phase shift upon transmission through the BS, as required by reciprocity (time-reversal invariance and parity conservation) [8]. Without loss of generality, we assume that the phase differential between the two paths in Fig. (1) is represented in the single parameter φ of the PS. Hence, for the configuration of Fig. (1), we have $\hat{\mathbf{T}}=\hat{\mathbf{P}}\hat{\mathbf{R}}\hat{\mathbf{B}}$. From the matrix equation relating input to output, we now deduce the output operators as $\hat{c}=(\hat{a}-i\hat{b})e^{i\varphi}/\sqrt{2}$ and $\hat{d}=(-i\hat{a}+\hat{b})/\sqrt{2}$, with similar expressions for their Hermitian conjugates. Hence, the total, scaled, electric-field annihilation operator $\hat{e}$, at the imaging plane of the lithographic substrate, is given by

$$\hat{e} = \hat{c} + \hat{d} = \frac{\left(-i + e^{i\varphi}\right)\hat{a} + \left(1 - ie^{i\varphi}\right)\hat{b}}{\sqrt{2}}\ , \tag{2}$$

with a conjugate expression for the creation operator. Here, the entire path differential between the upper and lower branches is contained in the phase factor $\varphi = 2kx$, where x is the lateral dimension on the imaging plane for grazing incidence. Now, to compute the normalized, two-photon, exposure dosage $\Delta_{2\gamma}$ from this quantum optics point of view, it is sufficient to compute the quantum expectation values of the moments of $\hat{e}$ and $\hat{e}^{\dagger}$. In particular, the one-, two-, and three-photon absorption rates at the imaging surface will be proportional to the expectation values of the following absorption dosing operators, $\hat{\delta}_1 = \hat{e}^{\dagger}\hat{e}$, $\hat{\delta}_2 = \hat{e}^{\dagger}\hat{e}^{\dagger}\hat{e}\hat{e}/2!$, and $\hat{\delta}_3 = \hat{e}^{\dagger}\hat{e}^{\dagger}\hat{e}^{\dagger}\hat{e}\hat{e}\hat{e}/3!$, respectively. The quantum theory of uncorrelated two-photon absorption was first worked out in 1931 by Maria Göppert-Mayer [9]. More recently, Javanainen and Gould [10] reported the equivalent theory for entangled two-photon absorption, while Perina, Saleh, and Teich [11] developed the entangled N-photon theory. The general N-photon deposition rate is

$$\hat{\delta}_N = \left(\hat{e}^{\dagger}\right)^N \left(\hat{e}\right)^N / N! \tag{3}$$

where the $N!$ is a normalization factor that arises from the bosonic enhancement factor, which is a result of the simple fact that the expectation value $\langle N | \left(\hat{e}^{\dagger}\right)^N \left(\hat{e}\right)^N | N \rangle = N!$ Hence, this normalization is required to prevent the over-counting of physically identical absorption processes, whereby N photons are

distributed over N virtual transitions in $N!$ different ways. All combinations lead to the same final (single) N-photon absorption process [12]. The expectation values are taken with respect to various input states that are allowed to enter the two-port system at the left of Fig. (1). The advantage of this operator-based approach is that all of the properties of the interferometer are encoded into the operator form of Eq. (2), and one may then use different input states without having to recalculate the effects of the interferometer over for each new input state [6]. Important for this work is the realization that the use of entangled photon states in interferometers have been shown to give a sub-shotnoise resolution capability [5–7]. What is new here is our recognition that this quantum resolution can be directly translated into a sub-diffraction-limited imaging or writing process, such as that employed by optical lithography.

Let us consider the input state $|\psi_I\rangle = |1\rangle_A|0\rangle_B$, for which uncorrelated photons are incident one-at-a-time from the left in the upper-left port A, with vacuum entering in lower-left port B (see Fig. 1). For this state we have the normalized expected deposition rate of $\Delta_{1\gamma}(\varphi) = \langle\psi_I|\hat{\delta}_1|\psi_I\rangle = 1-\sin\varphi = 1+\cos\left(\varphi+\frac{\pi}{2}\right)$, which is the usual classical result, up to an unimportant, constant, phase shift. (Since the photons are uncorrelated, the interference pattern is the same as for, say, a classical-like coherent input of the form $|\alpha\rangle_A|0\rangle_B$, as pointed out in Ref. 7.) Notice that $\Delta_{1\gamma}(\varphi)$ has a peak value of two, a minimum of zero, and a mean value of one, which normalizes the energy deposited per unit length to unity. The "classical" (uncorrelated) two-photon deposition rate is then the renormalized square of the one-photon rate, $\Delta^c_{2\gamma} = (1+\cos\varphi)^2/2 = \frac{3}{4}+\cos\varphi+\frac{1}{4}\cos 2\varphi$, where the

constant phase factor has been dropped. Recall that we wish to use quantum interference to delete the slowly varying middle $\cos\varphi$ term that appears here. A simple choice of a highly nonclassical number-product state accomplishes this, namely, the two-photon state $|\psi_{II}\rangle = |1\rangle_A |1\rangle_B$. This state is the natural output of a single-photon parametric down-conversion event [4]. The deposition rate on a two-photon absorbing substrate for this state, in the interferometric configuration of Fig. (1), has the form

$$\Delta_{2\gamma}^{q} = \langle \psi_{II} | \hat{\delta}_2 | \psi_{II} \rangle = 1 + \cos 2\varphi, \tag{4}$$

as desired. In other words, the middle term containing the more slowly oscillating $\cos\varphi$ has been deleted, and we are left with only the high-frequency $\cos 2\varphi$ term with the resolution of $x_{2\gamma}^{\min} = \lambda / 8$. Fig. (2), we plot the classical one-photon pattern, the classical two-photon pattern, and the entangled two-photon result.

To understand the physics behind this improvement—and the role of entanglement—we adapt a simple argument used by Huelga, *et al.,* in the context of Ramsey, atomic-clock, frequency measurements [13]. (A two-port Mach-Zehnder interferometer is isomorphic to a two-pulse Ramsey atomic-clock interferometer, via the SU(2) spinor rotation group [5].) Important to note is the form of the quantum state inside the interferometer in Fig. (1), after the beam splitter (BS) but before the phase shifter (PS), at the points A′ and B′. It is well known that, upon passage through a symmetric, lossless beamsplitter, the product number state $|\psi_{II}\rangle = |1\rangle_A |1\rangle_B$ becomes an entangled number state of the

form $|\psi_E\rangle = \left(|0\rangle_{A'}|2\rangle_{B'} + |2\rangle_{A'}|0\rangle_{B'}\right)/\sqrt{2}$, due to interference at the beamsplitter itself [5]. Here, the entanglement is between number and path; it is not possible to tell, even in principal, whether *both* photons took the lower-most path or *both* took the upper-most path. This entangled state is sometimes called a "diphoton" or a "two-photon", and it behaves as single quantum object of photon number two in a spatially separated superposition state [14]. There are two indistinguishable paths—up or down—this diphoton can take through the interferometer, and so the quantum amplitudes corresponding to these two paths will add and interfere. However, the diphoton will pass through the phase shifter only on the upper-most path, and hence this amplitude will acquire twice the phase shift as with a single photon process. Therefore, it is easy to see that the entangled state becomes, $|\psi_E(\varphi)\rangle = \left(|0\rangle_C|2\rangle_D + e^{2i\varphi}|2\rangle_C|0\rangle_D\right)/\sqrt{2}$. Hence, the entangled quantum state inside the interferometer accumulates phase twice as fast as would occur with an uncorrelated photon pair. This is the origin of the doubling of the resolution, found implicitly in the deposition rate, Eq. (4), which could equally well be computed as $\langle\psi_E(\varphi)|\left(\hat{c}^\dagger + \hat{d}^\dagger\right)^2\left(\hat{c} + \hat{d}\right)^2|\psi_E(\varphi)\rangle$. It is a simple matter to show, in analogy to the atomic-clock work of Huelga, *et al.,* that if an entangled photon number state of the form

$$|\psi_E(N)\rangle = \left(|0\rangle_{A'}|N\rangle_{B'} + |N\rangle_{A'}|0\rangle_{B'}\right)/\sqrt{2}, \tag{5}$$

is prepared inside the interferometer, then the phase from the path differential accumulates N times as fast, producing an entangled state of the form $|\psi_E(N)\rangle = \left(|0\rangle_C|N\rangle_D + e^{iN\varphi}|N\rangle_C|0\rangle_D\right)/\sqrt{2}$ at the output. If the substrate in this case is an N-

photon absorbing material, then the deposition function $\hat{\delta}_N$, Eq. (3), has an expectation value equal to,

$$\langle \psi_E(N,\varphi) | \left(\hat{c}^\dagger + \hat{d}^\dagger\right)^N \left(\hat{c} + \hat{d}\right)^N | \psi_E(N,\varphi) \rangle = 1 + \cos N\varphi \ , \tag{6}$$

where all the slowly oscillating terms have been interferometrically deleted from the pattern. This selective deletion of the undesirable cross terms is a consequence of the use of nonclassical number states—a similar result can not be had using coherent states [7]. The result leaves only the fastest varying term of $\cos N\varphi$, which then writes a pattern that has a feature size resolution of $\lambda/(4N)$. This is a remarkable factor of N below the classical Rayleigh limit of $\lambda/4$.

Of course, the natural question arises: how can one produce maximally entangled photon number states of the form given in Eq. (5)? For the case of $N = 2$, the answer is a parametric down-conversion event, followed by a symmetric beamsplitter. For higher N, there are at several possibilities. One approach is to use a material with a $\chi^{(N)}$ nonlinearity, in which a single photon is downconverted into N entangled daughter photons, as discussed by Perina, Saleh and Teich [12]. Another approach is to utilize a cascaded arrangement of N–1 crystals with $\chi^{(2)}$ nonlinearities [12,16]. It is interesting to note that the natural output of a series of parametric downconversion events, or that of an optical parametric oscillator (OPO), has the form $|N/2\rangle_A |N/2\rangle_B$ of a Hilbert space product [6,7]. In the case $N = 2$, a simple linear beam splitter can be used to generated the maximally entangled form of Eq. (5) from this state.

We make one final important note on the entangled N-photon absorption process. Classically, the uncorrelated N-photon absorption probability scales like I^N, where I is the normalized classical intensity. This result is a consequence of the fact that the photons arrive independently of each other. Hence, the probability that the first photon arrives in an elemental absorption volume in space-time is proportional to I, and the probability a second photon will also happen to be in the same volume is also proportional to I, and so on, giving the I^N law. For this reason, N-photon absorption lithography with uncorrelated "classical" light is unfeasible for high N, since extremely high flux densities are required [12]. This is not the case for N-photon absorption with entangled photons. Javanainen and Gould first demonstrated that for two-photon absorption with entangled photon pairs, the absorption cross section scales as I, and not the I^2 that would be expected classically [11]. Later on, Perina, Saleh, and Teich showed that this holds for arbitrary N, namely, that the N-photon absorption cross-section, with N entangled photons, scales like I and not I^N [12]. This result can be seen by the following heuristic argument: Recall that the photons are correlated in space and time, as well as number. Hence, if the optical system is aligned properly, the probability of the first photon arriving in a small absorptive volume of spacetime is proportional to I. However, the remaining N–1 photons are constrained to arrive at the same place at the same time, and so each of their arrival probabilities is a constant, independent of I. Hence, although classical N-photon lithography requires unrealistically high optical powers, entangled N-photon lithography requires only the same levels of power as the classical one-photon device.

In conclusion, we have discussed the problem of entangled N-photon absorption, as applied to interferometric optical lithography. We conclude that maximally entangle photon states, such as in Eq. (5), can be used to write features in an N-photon absorbing resist which have a resolution of $\lambda/(4N)$. This result is a factor of N below the classical Rayleigh limit. Such states can easily be made for $N=2$ using optical parametric downconversion, and there are several possible approaches for implementing the scheme for higher N. It is remarkable to note that entanglement is a useful resource, which can be employed in a technology such as lithography to overcome seemingly unbreakable constraints such as the diffraction limit. The classical limit is not that which is imposed by quantum mechanics.

ACKNOWLEDGEMENTS

We would like to acknowledge interesting and useful discussions with R. Y. Chiao, J. D. Franson, P. W. Kwiat, A. Scherer, M. O. Scully, J. E. Sipe, R. B. Vrijen, and E. Yablonovitch. The research described in this paper was carried out by the Jet Propulsion Laboratory, California Institute of Technology, under a contract with the National Aeronautics and Space Administration.

REFERENCES

1. A. Hawryliw, Microelectron. Eng. **35**, 11 (1997).

2. S. R. J. Brueck, *et al.,* Microelectron. Eng. **42**, 145 (1998).

3. Lord Rayleigh, Phil. Mag. **8**, 261 (1879); M. Born and E. Wolf, *Principles of Optics,* 6th ed. (Pergamon Press, New York, 1980), Sec. 7.6.3.

4. E. Yablonovitch and R. B. Vrijen RB, Opt. Eng. **38**, 334 (1999).

5. C. K. Hong and L. Mandel, Phys. Rev. A **31**, 2409 (1985);

6. B. Yurke, Phys. Rev. Lett. **56**, 1515 (1986); M. Hillery, *et al.,* Quantum Semicla. Opt. **8**, 1041 (1996); T. Kim *et al.,* Phys. Rev. A **57**, 4004 (1998).

7. J. P. Dowling, Phys. Rev. A **57**, 4736 (1998).

8. A. Kuzmich and L. Mandel, Quantum Semicl. Opt. **10**, 493 (1998); E. J. S. Fonseca, *et al.,* Phys. Rev. A **60**, 1530 (1999).

9. J. P. Dowling, IEE Proceedings - Optoelectronics **145**, 420 (1998).

10. M. Göppert-Mayer, Ann. Phys. **5**, 273 (1931).

11. J. Javanainen and P. L. Gould, Phys. Rev. A **41**, 5088 (1990).

12. J. Perina Jr., B. E. A. Saleh, and M. C. Teich, Phys. Rev. A **57**, 3972 (1998).

13. M. Hillery, Phys. Rev. A **42**, 498 (1990).

14. S. F. Huelga, *et al.,* Phys. Rev. Lett. **79**, 3865 (1997).

15. I. H. Deutsch, R. Y. Chiao, and J. C. Garrison, Phys. Rev. A **47**, 3330 (1993); T. B. Pittman, *et al.,* Phys. Rev. Lett. **77**, 1917 (1996).

16. T. E. Keller, M. H. Rubin, and Y. Shih, Phys. Rev. A **57**, 2076 (1998).

FIGURE CAPTIONS

Fig. 1 The interferometric lithography set up for utilizing photons entering ports A and B, entangled two at a time. The photons strike the symmetric, lossless, beamsplitter (BS) and then reflect off the mirrors (M). The photon amplitude in the upper path accumulates at the phase shifter (PS) a phase shift φ before the two branches are made to interfere on the substrate.

Fig. 2 This plot compares the deposition pattern Δ as a function of the phase shift φ for uncorrelated single-photon absorption (dashed), uncorrelated two-photon absorption (dotted), and entangled two-photon absorption (solid). Note that the classical two-photon plot has narrower features than the one-photon, but that the entangled two-photon has even narrower features still. In addition, the entangled profile also shows the critical halving of the peak-to-peak separation.

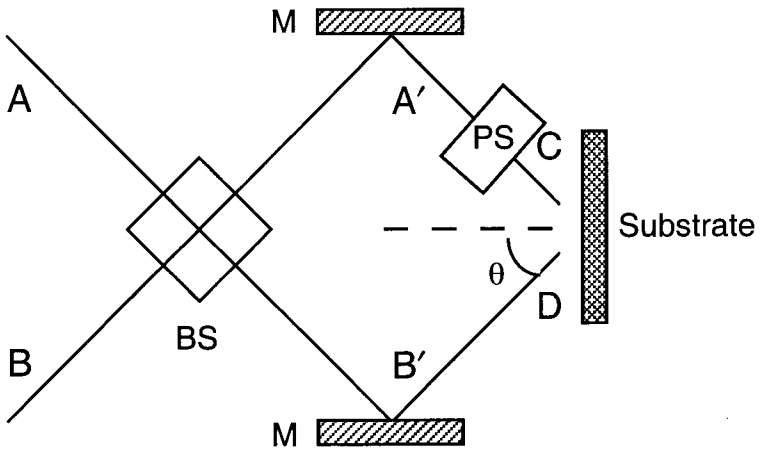

Fig. 1

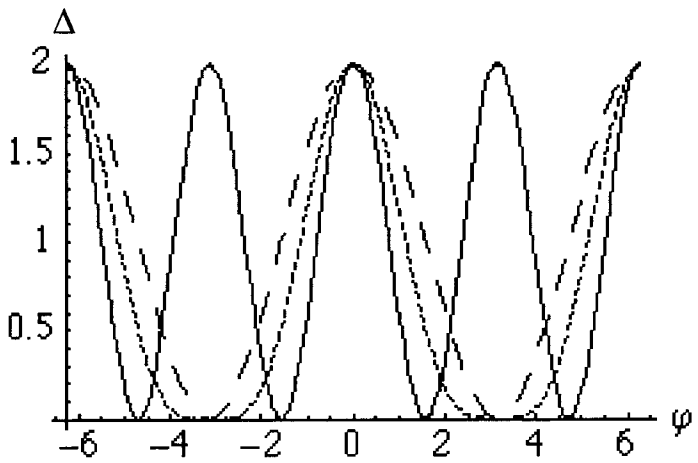

Fig. 2